Sensors and Materials, Vol. 11, No. 5 (1999) 257–267
MYU Tokyo

S & M 0370

Investigation on Sensing Properties of ZnO-Based Thin Film Sensors for Trimethylamine Gas

Tae Ha Kwon, Jee Youl Ryu, Woo Chang Choi, Sung Woo Kim, Sung Hyun Park, Hyek Hwan Choi and Myong Kyo Lee

Department of Electronics, Pukyong National University, Pusan, 608-737, Korea

(Received December 10, 1998; accepted July 22, 1999)

Key words: TMA gas, ZnO-based thin film sensors, sputtering, Hall effect, AES, XRD, sensitivity

The sensing properties of ZnO-based thin film sensors for trimethylamine (TMA) gas were investigated. ZnO-based thin films for use as sensors were deposited by a RF magnetron sputtering method. We examined the effects of various metal oxide additives and sputtering gases on ZnO-based thin film. To improve the stability of the electrical resistance of the thin films, heat treatment at 330°C in oxygen was carried out for 72 h. To investigate the sensing properties for TMA gas, we measured the Hall effect, and analyzed the Auger electron spectroscopy (AES) and X-ray diffraction (XRD) results. The ZnO-based sensor was fabricated using thin film sputtered in oxygen and codoped with 4.0 wt.% Al_2O_3, 1.0 wt.% TiO_2, 1.0 wt.% In_2O_3 and 0.2 wt.% V_2O_5. This sensor showed the highest sensitivity of 264 at the working temperature of 300°C for 160 ppm TMA gas. Its surface carrier concentration was 2.96×10^{23} cm^{-3} and its Hall electron mobility was 18 cm^2/Vs.

1. Introduction

Trimethylamine (TMA) gas sensors using metal oxide semiconductors such as ZnO, TiO_2, Al_2O_3 and In_2O_3 are very useful for the evaluation of fish freshness and in various fields of the food industry.[1–10] To evaluate fish freshness, the most widely used method is based on the chemical analysis of decomposition products from adenosine triphosphate

(ATP)-related compounds in the tissue of fish, but this method is destructive and requires much time and effort.[1–7] It is imperative to develop a rapid, accurate, continuous, and nondestructive method for evaluating fish freshness. Such a method must be realized using a semiconductor gas sensor which responds to changes in the concentration of TMA, dimethylamine (DMA) or ammonia gas emitted during the decomposition of fish. It is known that gas sensors using ZnO thin films have good sensitivity and excellent selectivity to TMA, DMA or ammonia gas, and they can be used to monitor the fish freshness in a rapid, accurate, and nondestructive manner.[1–5,11–19] To fabricate these sensors, it is necessary to investigate the factors which affect the improvement of sensor properties such as sensitivity, selectivity and electrical stability.

In this study, the sensing properties of ZnO-based thin film sensors for TMA gas were investigated. The ZnO-based thin films for use as sensors were deposited by a RF magnetron sputtering method. The effects of various metal oxide additives and sputtering gases on ZnO-based thin film were examined. The heat treatment at 330°C in oxygen was carried out for 72 h to improve the stability of the electrical resistance of the thin films. To investigate the sensing properties for TMA gas, the Hall effect was measured, and the Auger electron spectroscopy (AES) and X-ray diffraction (XRD) results were analyzed.

2. Experiment

2.1 *Sample preparation*

Nine targets were prepared using ZnO, Al_2O_3, TiO_2, In_2O_3, and/or V_2O_5 powders. To investigate the sensing properties of the ZnO thin film sensor and ZnO-based thin film sensors with additives, one target was composed of pure ZnO powder and the others were codoped with Al_2O_3, TiO_2, In_2O_3, and/or V_2O_5. The films were fabricated using these targets by the RF magnetron sputtering method at an argon and/or oxygen gas pressure of 10^{-2} Torr. The sputtering conditions for ZnO-based thin films and the series of sensors fabricated under different conditions are shown in Tables 1 and 2, respectively.

To improve the stability of the electrical resistance of as-deposited films, they were aged in a furnace at 330°C for 72 h in oxygen. The films were then exposed to air for 30 days.

Table 1.
Sputtering conditions for ZnO-based thin films.

RF power	120 W
Substrate	$Si_3N_4/SiO_2/Si_3N_4/Si$ (2×2×0.6 mm^3)
Substrate temperature	250°C
Target material	ZnO, Al_2O_3, TiO_2, In_2O_3, V_2O_5 powders (99.99% purity)
Base vacuum	1×10^{-6} Torr, 1×10^{-5} Torr (250°C)
Gas pressure	10 mTorr
Atmospheric gas (sccm)	O_2:Ar = 1:0, 1:1, 0:1
Deposition rate	100 – 120 Å/min
Cooling	Natural cooling

Table 2.
Sensors fabricated under different conditions.

Sensors	Catalytic additives and weight ratio (wt.%) of the targets
# 1	ZnO
# 2	$ZnO+Al_2O_3(2)$
# 3	$ZnO+Al_2O_3(4)$
# 4	$ZnO+Al_2O_3(6)$
# 5	$ZnO+TiO_2(1)$
# 6	$ZnO+TiO_2(3)$
# 7	$ZnO+Al_2O_3(4)+TiO_2(1)$
# 8	$ZnO+Al_2O_3(4)+TiO_2(1)+V_2O_5(0.2)$
# 9	$ZnO+Al_2O_3(4)+In_2O_3(1)+TiO_2(1)+V_2O_5(0.2)$

To control the working temperature of the sensor, the Pt (99.99% purity) heater was also fabricated by RF magnetron sputtering deposition for 30 min on a $Si_3N_4/SiO_2/Si_3N_4/Si$ substrate heated at 250°C at a pressure of 5 mTorr with RF power of 140 W in argon. Titanium (99.9% purity) was used as an adhesive layer. The Pt film was about 0.7 μm thick, 40 μm wide, and 25.92 mm long. To decrease the power dissipation, the back of the substrates was etched. The electrodes (Au, 0.5 μm thickness) were then deposited on each ZnO-based thin film. Figure 1 shows the cross-sectional view of the fabricated sensor.

2.2 *Sensitivity and Hall effect measurement*

The sensitivity (K) was defined as R_a/R_g, where R_a and R_g are the electrical resistances of the sensor in air and in TMA gas, respectively.[3,4] The working temperature of the sensor was controlled by adjusting the DC current flow in the Pt heater.

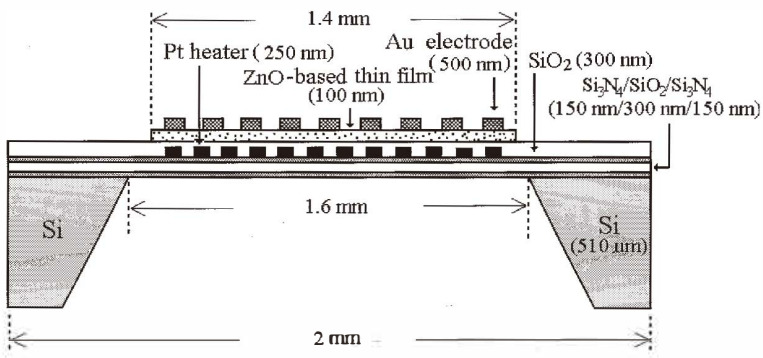

Fig. 1. Cross-sectional structure of the sensor.

The four-point electrode structure for the Hall effect measurement is shown in Fig. 2. The Hall voltage was measured with the current of 1 mA and magnetic flux density of 1–10 kG. The surface carrier concentration and Hall mobility were calculated from the Hall voltage measured.[8–12] The area of each electrode occupies one-tenth of the total active space of the films and the shape coefficient (G) is 0.675.[10]

The concentration of carriers at the surface n_s is given as

$$n_s = -\frac{GB_z I_x L r_n}{qwt_0 V_{Hm}} = \frac{\sigma_n}{q\mu_{Hn}}, \tag{1}$$

where r_n (theoretical values: r_n=1.18 for phonon scattering and r_n=1.93 for impurity scattering) denotes the scattering factor,[10] q is the electronic charge, t_0 is the thickness of the space-charge layer, σ_n is the surface conductivity, and μ_{Hn} is the Hall mobility.

The Hall mobility μ_{Hn} is given by

$$\mu_{Hn} = \frac{\mu_i \mu_g}{\mu_i + \mu_g} = r_n \mu_n = \frac{V_{Hm}}{r_n R G I_x B_z}, \tag{2}$$

where μ_i and μ_g are the Hall mobilities for impurity scattering and grain boundary scattering, respectively.

The sensitivity K is given by

$$K = R_a / R_g = n_g / n_s = \rho_n / \rho_g = V_{Hm} / V_{Hm(g)}, \tag{3}$$

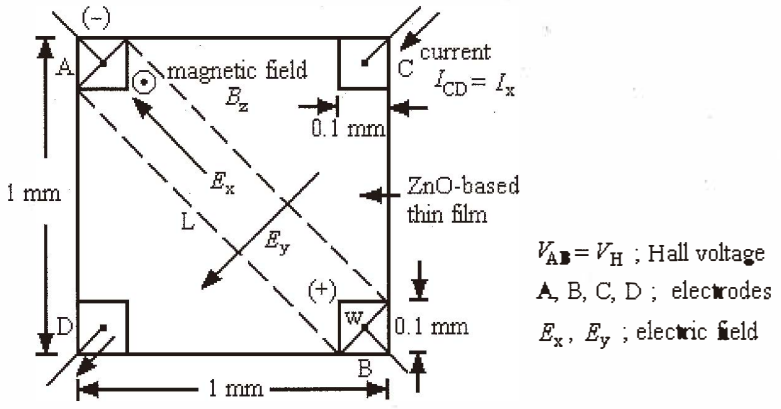

Fig. 2. Four-point electrode structure for Hall effect measurement.

where R_a is the resistance in air, and R_g, n_g, ρ_g and $V_{Hm(g)}$ are the resistance, carrier concentration, resistivity and Hall measurement voltage for TMA, respectively.

2.3 *AES and X-ray investigations*

We have used the Perkin-Elmer PHI 650 AES to investigate the effects of the sputtering gas and additives. Crystalline phase structure of the thin films was analyzed using a Rigaku DMAX-2500 X-ray diffractometer with Cu $K\alpha 1$ radiation in the usual $\theta - 2\theta$ geometry.

3. Results and Discussion

3.1 *Sensitivity, Hall mobility, carrier concentration and resistivity*

The data on the electrical properties were obtained at the working temperature of 300°C in 160 ppm TMA or in air for the sensors, as summarized in Table 3. Sensor #9 was the most sensitive to TMA, its sensitivity to 160 ppm TMA at 300°C being 264. When Al_2O_3, In_2O_3, TiO_2 and V_2O_5 were codoped to ZnO, the sensitivity increased markedly. This result shows that Al_2O_3, In_2O_3, TiO_2 and V_2O_5 are effective promoters of sensitivity to TMA and are used to accelerate the chemical reaction between TMA gas and oxygen adsorbates on ZnO-based thin films. Based on these finding, we can assume that Al, In, Ti and V act as effective donors in ZnO. As the working temperature increases, the sensitivity increases up to 300°C, and then decreases above 300°C. When the temperature is varied with a given concentration of TMA gas, a peak usually appears in the sensitivity versus temperature plot. If the temperature is too low, the overall reduction reaction is too slow to give a high sensitivity, whereas if the temperature is too high, the overall oxidation reaction proceeds so rapidly that the concentration of TMA gas at the surface becomes diffusion-limited and

Table 3. Electrical properties of sensors.
(Working temperature, 300°C; TMA gas concentration, 160 ppm; I_x=1 mA; B_Z=1 kG)

Sensors	Parameter										
	R (Ω)		$V_{Hm}\times10^{-1}$ (mV)		$n_s\times10^{21}$ (cm^{-3})		$\rho_n\times10^{-5}$ (Ωm)		μ_{Hn} (cm^2/Vs)		K
	in air	in TMA	in air	in TMA	in air	in TMA	in air	in TMA	in air	in TMA	
# 1	2,800	37.33	−47.20	−6.30	0.13	9.80	60.00	0.80	80.30	80.30	75.00
# 2	2,400	14.30	−14.30	−0.20	0.46	32.20	48.00	0.69	28.40	28.40	70.00
# 3	2,040	24.90	−11.14	−0.14	0.57	46.93	42.00	0.51	26.00	26.00	82.00
# 4	2,600	38.24	−16.54	−0.24	0.65	44.00	51.00	0.75	30.30	30.30	68.00
# 5	3,200	47.80	−22.90	−0.34	0.29	19.24	64.00	0.96	34.00	34.00	67.00
# 6	3,550	61.20	−28.70	−0.50	0.23	13.30	71.00	1.22	38.50	38.50	58.00
# 7	1,700	12.50	−79.00	−0.06	0.84	113.70	34.00	0.25	22.00	22.00	136.00
# 8	1,800	11.40	−78.00	−0.05	0.84	133.20	36.00	0.23	20.60	20.60	158.00
# 9	1,550	5.90	−59.00	−0.02	1.12	295.70	31.00	0.12	18.00	18.00	264.00

R = sensor resistance, V_{Hm} = Hall measurement voltage, n_s = carrier concentration,
ρ_n = electrical resistivity, μ_{Hn} = Hall mobility, K = sensitivity.

the sensitivity again is low.[12]

It can also be seen that doped sensors #2 to #9 exhibit high carrier concentration, and low Hall mobility and electrical resistivity in comparison with those of nondoped sensor #1. The high carrier concentration of ZnO thin films codoped with Al_2O_3, TiO_2, In_2O_3 and V_2O_5 is expected due to the contribution of doped ions such as Al^{+3}, Ti^{+4}, In^{+3} and V^{+5} on substitutional sites of Zn^{+2} ions and/or from their interstitial atoms in the ZnO lattice, as well as from oxygen vacancies and/or interstitial zinc atoms.[12] It has been reported that an Al- or In-doped ZnO film has high carrier concentration, low resistivity, and stable electrical properties as compared with a nondoped ZnO film.[13] TiO_2 is also expected to be incorporated in the lattice. V_2O_5 has also been shown to have the effect of stabilizing the electrical resistance.[3–5] The ZnO films codoped with additives showed lower Hall mobility than nondoped films. It is shown that the mobility decreases with increasing impurity content due to not only the carrier concentration dependence of ionized impurity scattering but also the enhancement of both grain boundary scattering and ionized impurity scattering resulting from the disorder introduced in the ZnO lattice.[11] The decrease of the mobility of ZnO films doped with additives can be roughly explained in terms of the increase of the degree of disorder introduced in the ZnO lattice and of the carrier concentration, which correlate to the increase of the ion radius of impurity atoms.

Figure 3 shows the sensing and electrical properties of sensor #9 (sputtering in O_2) vs various working temperature in 160 ppm TMA gas or in air. Sensor #9 codoped with

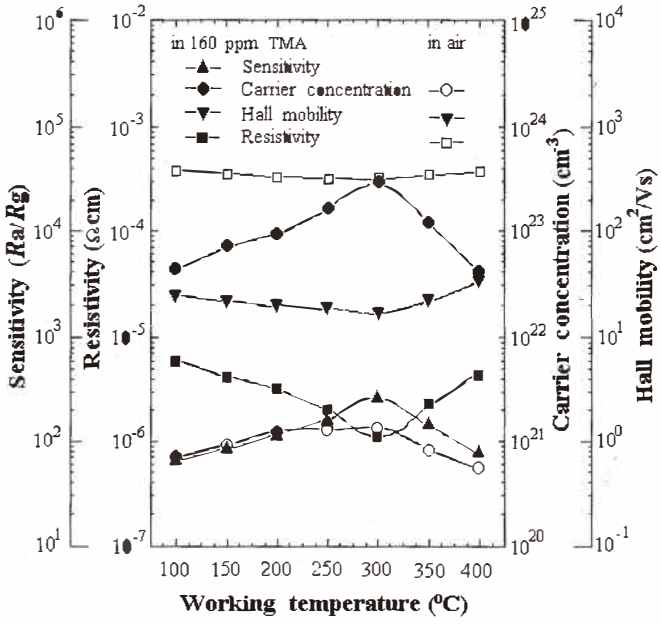

Fig. 3. Sensing and electrical properties of sensor #9 (sputtering in O_2) vs working temperature.

additives showed a high sensitivity of 264 to 160 ppm TMA at 300°C. The Hall mobility was not affected by TMA gas. We suggest that the mobility of doped film decreases with increasing temperature up to 300°C due to both grain boundary scattering (e.g., lattice scattering), which causes ever-increasing thermal agitation of the ZnO atoms, and ionized impurity scattering,[11] and increases above that temperature. Sensor #9 exhibited the low Hall mobility of 18 cm^2/Vs at 300°C. In a TMA gas, the carrier concentration of the films was obviously increased, as explained in refs. 9 and 13.

The sensing and electrical properties of sensor #9 for various sputtering gas atmospheres in 160 ppm TMA or in air are shown in Fig. 4. The sensor fabricated with thin films sputtered in oxygen showed higher sensitivity than those sputtered in argon or in oxygen/argon. The oxygen gas used in sputtering reduces the deposition rate and compensates the defects of the lattice oxygen.[9] It is believed that the improvement of the film sensitivity is due to the oxygen gas used in sputtering.

The results in Figs. 3 and 4 confirm that the enhanced sensitivity can be attributed to the increase of the carrier concentration, and the decrease of the Hall mobility and resistivity, as suggested by eqs. (1) and (2). In view of the above results, two points are especially deserving of notice. First, we can suggest that each doped additive markedly affects the increase of the carrier concentration and the sensitivity, and the decrease of the Hall mobility. Second, we can consider that the oxygen gas used in sputtering affects the increase of the carrier concentration and the sensitivity, and the decrease of the Hall mobility.

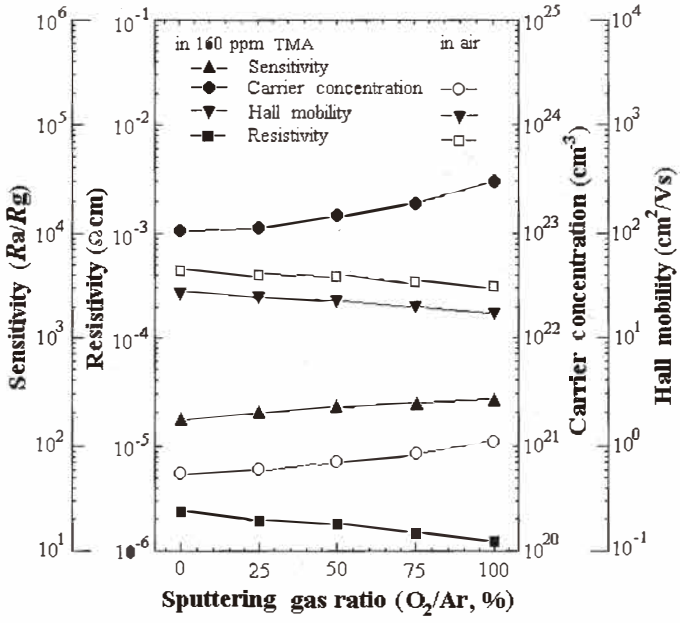

Fig. 4. Sensing and electrical properties of sensor #9 vs sputtering gas ratio.

3.2 *AES and XRD analyses*

We have investigated the effects of sputtering gas and additives using AES. The patterns, obtained by AES surface analysis, for the thin films are shown in Figs. 5(a) and 5(b). The peak of Zn and/or additive elements (e.g., Al, Ti, In, V), as shown in Fig. 5, was examined. In particular, it can be seen that thin films doped with additives consist of a more suitable balance between the atomic concentration ratios for Zn and for oxygen than the nondoped films.

Figures 6(a) and 6(b) show the AES depth profile for the thin films. The ZnO-based thin films doped with additives and sputtered in O_2 had better uniformity than the nondoped films sputtered in Ar. In addition, it can be inferred that sensor #9 (sputtering in O_2) has higher carrier density and/or higher compaction due to a longer sputter time, as shown in Fig. 6(b). From the results in Figs. 5 and 6, even if the enhanced sensitivity of sensor #9 cannot be fully justified, we can infer that its sensitivity improvement can be attributed to the decrease of the mobility due to the good uniformity of the film.[9]

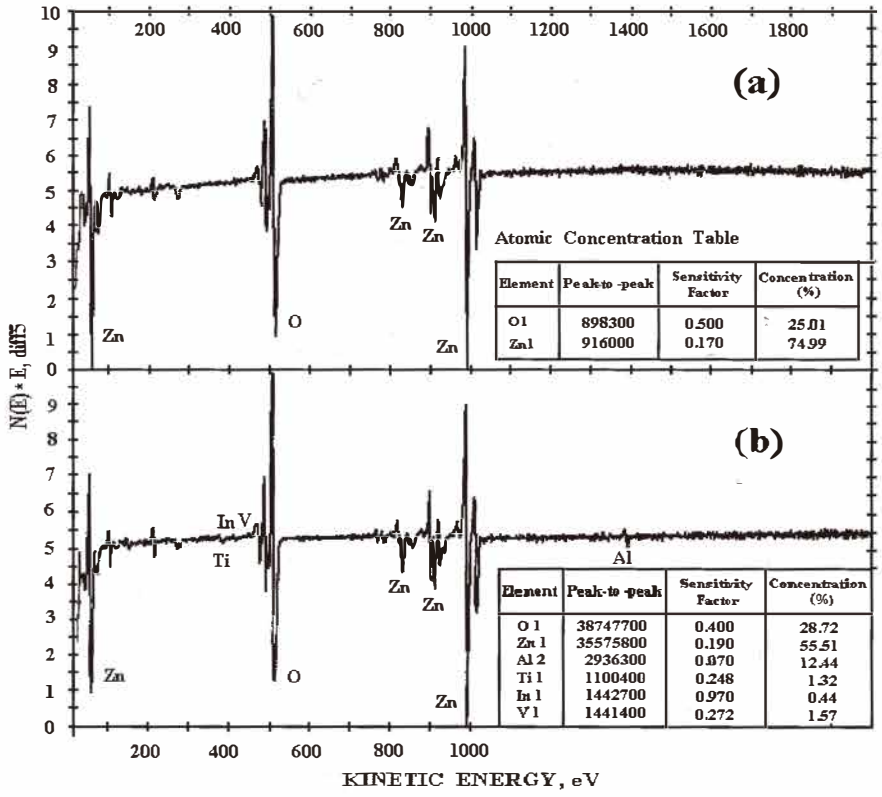

Fig. 5. Patterns, obtained by AES surface analysis, for the thin films. (a) #1 (sputtering in Ar), (b) #9 (sputtering in O_2).

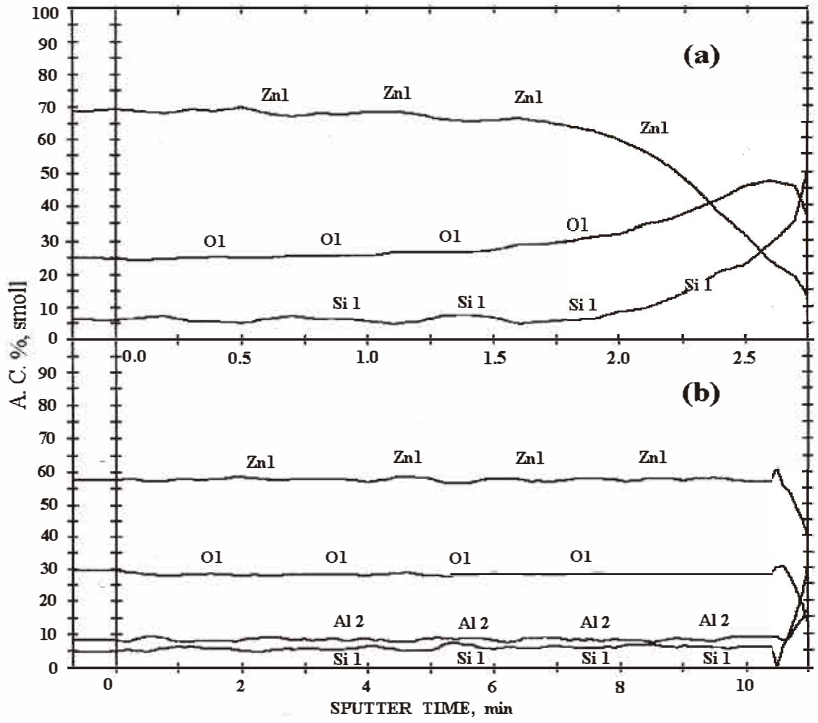

Fig. 6. AES depth profile of the thin films. (a) #1 (sputtering in Ar), (b) #9 (sputtering in O_2).

Figures 7(a) and 7(b) show the 2θ XRD patterns for the films. It is well known that sputtered ZnO-based thin films are highly textured with the *c*-axis perpendicular to the substrate surface.[20,21] The XRD spectra are dominated by the (002) diffraction peak at $2\theta \approx 34$ degrees for ZnO-based thin films confirming the strong (001) texture of these films in comparison to the strong (101) peak at $2\theta \approx 36$ degrees in the JCPDS file card (36-1451). A sharp (002) peak at $2\theta \approx 34$ degrees indicates that the films are polycrystalline ZnO with the *c*-axis perpendicular to the substrate surface (*c*-axis orientation).[22] Sensor #1 sputtered in Ar showed also strong (002) and weak (201), (100), (101) peaks, while sensor #1 sputtered in O_2 showed a relatively strong (201) peak at $2\theta \approx 69$ degrees, as shown in Fig. 7(a). It may be inferred that because sensor # 1 sputtered in O_2 has randomly oriented grains along the surface normal,[20,21] this sensor shows a relatively strong (201) peak at $2\theta \approx 69$ degrees. However, it should be stated that the reason for this behavior is not clear at present. After adding the various metal oxide additives, the weak (100) peak was not observed and sensor #9 sputtered in O_2 showed a relatively strong (002) peak at $2\theta \approx 34$ degrees, indicating a role of additives as a mineralizer or surfactant that significantly improves the texture of the layers.[21] From the results in Fig. 7, even if the enhanced

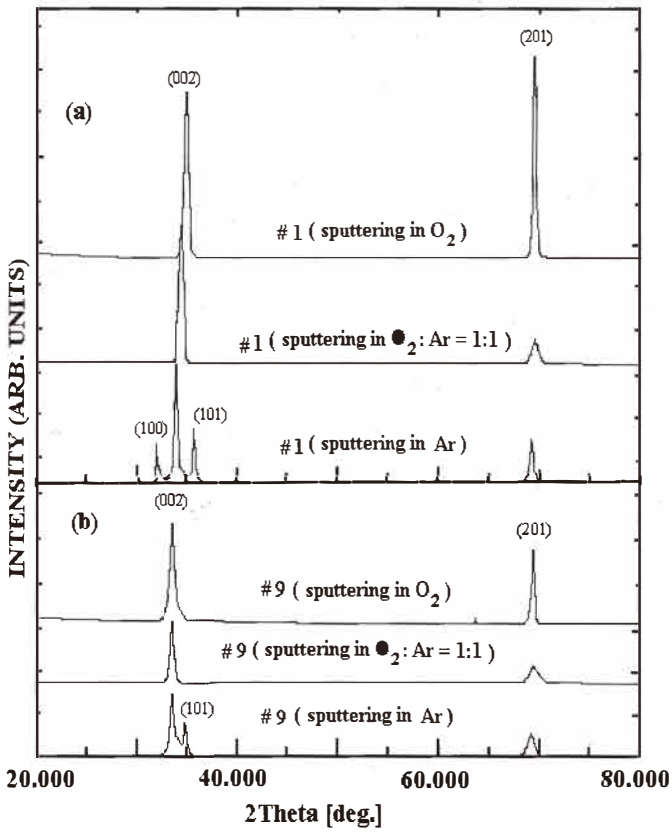

Fig. 7. XRD pattern for the thin films.

sensitivity of sensor #9 cannot be fully justified, we can assume that improvement of the sensitivity can be attributed to the highly textured *c*-axis orientation.

4. Conclusions

ZnO-based thin films were fabricated by a RF magnetron sputtering method. To improve the stability of the electrical resistance of the thin films, they were heat-treated at 330°C for 72 h in oxygen. We examined the effects of various metal oxide additives and sputtering gases, and carried out the Hall effect measurement, AES, and XRD analyses to investigate the sensing and electrical properties of ZnO-based thin film sensors for TMA gas.

The ZnO-based sensor fabricated with the thin film sputtered in oxygen and codoped with 4.0 wt.% Al_2O_3, 1.0 wt.% TiO_2, 1.0 wt.% In_2O_3 and 0.2 wt.% V_2O_5 exhibited the highest sensitivity (264) at the working temperature of 300°C for 160 ppm TMA gas. The surface carrier concentration of this sensor was 2.96×10^{23} cm^{-3} and its Hall electron mobility was 18 cm^2/Vs. The ZnO-based thin films doped with additives had better uniformity than the nondoped films. From XRD analysis, we could assume that improvement of the sensitivity can be attributed to the highly textured *c*-axis orientation.

References

1 M. Egashira, Y. Shimizu and Y. Takao: Sensors and Actuators B **1** (1990) 108.
2 H. Nanto, H. Sokooshi and T. Kawai: Sensors and Actuators B **13–14** (1993) 715.
3 J. Y. Ryu, S. H. Park, H. H. Choi, M. K. Lee and T. H. Kwon: J. Korean Sensors Society **6** (1997) 265.
4 J. Y. Ryu, S. H. Park, H. H. Choi and T. H. Kwon: J. Korea Institute of Telematics and Electronics **34** (1997) 1016.
5 S. H. Park, H. H. Choi and T. H. Kwon: Sensors and Materials **8** (1996) 485.
6 J. C. Yen: J. Vac. Sci. Technol. **12** (1975) 47.
7 L. Ristic: Sensor Technology and Devices (1994) 30-33, 239, 242, 396-397.
8 H. Ohnishi, H. Sananki, T. Matsumoto and M. Ipponmatsu: Sensors and Actuators B **13–14** (1993) 677.
9 S. M. Sze: Chemical Sensors, Semiconductor Sensors **22** (1995) 383.
10 Th. Kwaaitaal: Sensors and Actuators A **39** (1993) 103.
11 T. Minami, H. Sato, H. Nanto and S. Takata: Jpn. J. Appl. Phys. **24** (1985) L781.
12 S. R. Morrison: Sensors and Actuators **12** (1987) 425.
13 T. Minami, H. Nanto and S. Takata: Jpn. J. Appl. Phys. **23** (1985) L280.
14 T. Minami, H. Nanto and S. Takata: Appl. Phys. Lett. **41** (1982) 958.
15 T. Minami, H. Nanto and S. Takata: Thin Solid Films **124** (1985) 43.
16 H. Nanto, T. Minami, S. Shooji and S. Takata: J. Appl. Phys. **55** (1985) 1029.
17 Y. Takao, Y. Iwanaga, Y. Shimizu and M. Egashira: Sensors and Actuators B **10** (1993) 229.
18 Y. Takao, K. Fukuda, Y. Shimizu and M. Egashira: Sensors and Actuators B **10** (1993) 235.
19 T. H. Kwon, S. H. Park, J. Y. Ryu and H. H. Choi: Sensors and Actuators B **46** (1998) 75.
20 F. C. Lin, Y. Takao, Y. Shimizu and M. Egashira: Sensors and Actuators B **24–25** (1995) 843.
21 R. Cebulla, R. Wendt and K. Ellmer: J. Appl. Phys. **83** (1998) 1087.
22 N. Tsuji, H. Komiyama and K. Tanaka: Jpn. J. Appl. Phys. **29** (1990) 835.